SAND2019-4185C

Proceedings of the ASME 2019 Pressure Vessels & Piping Conference
PVP 2019
July 14-19, 2019, San Antonio, TX, USA

PVP2019-93907

TECHNICAL BASIS FOR MASTER CURVE FOR FATIGUE CRACK GROWTH OF FERRITIC STEELS IN HIGH-PRESSURE GASEOUS HYDROGEN IN ASME SECTION VIII-3 CODE

Chris San Marchi
Sandia National Laboratories
Livermore, CA, USA

Joseph Ronevich
Sandia National Laboratories
Livermore, CA, USA

Paolo Bortot
Tenaris Dalmine
Dalmine, Italy

Yoru Wada
Japan Steel Works
Hokkaido, Japan

John Felbaum
FIBA Technologies
Littleton MA, USA

Mahendra Rana
Consultant
Niantic CT, USA

ABSTRACT

The design of pressure vessels for high-pressure gaseous hydrogen service per ASME Boiler and Pressure Vessel Code Section VIII Division 3 requires measurement of fatigue crack growth rates in situ in gaseous hydrogen at the design pressure. These measurements are challenging and only a few laboratories in the world are equipped to make these measurements, especially in gaseous hydrogen at pressure in excess of 100 MPa. However, sufficient data is now available to show that common pressure vessel steels (e.g., SA-372 and SA-723) show similar fatigue crack growth rates when the maximum applied stress intensity factor is significantly less than the elastic-plastic fracture toughness. Indeed, the measured rates are sufficiently consistent that a master curve for fatigue crack growth in gaseous hydrogen can be established for steels with tensile strength less than 915 MPa. In this overview, published reports of fatigue crack growth rate data in gaseous hydrogen are reviewed. These data are used to formulate a two-part master curve for fatigue crack growth in high-pressure (106 MPa) gaseous hydrogen, following the classic power-law formulation for fatigue crack growth and a term that accounts for the loading ratio (R). The bounds on applicability of the master curve are discussed, including the relationship between hydrogen-assisted fracture and tensile strength of these steels. These data have been used in developing ASME VIII-3 Code Case 2938. Additionally, a phenomenological term for pressure can be added to the master curve and it is shown that the same master curve formulation captures the behavior of pressure vessel and pipeline steels at significantly lower pressure.

INTRODUCTION

The ASME Boiler and Pressure Vessel Code Section VIII Division 3 requires fracture mechanics-based design for high-pressure hydrogen storage vessels using fatigue crack growth measurements performed in the service environment. For storage applications to support refueling of hydrogen fuel cell vehicles the service condition is pure gaseous hydrogen at pressure up to about 100 MPa. Until recently, the publicly available data to support these fatigue-based designs were summarized in just a handful of publications, in particular Refs. [1, 2]. Figure 1 summarizes the data from these two references, which includes fatigue crack growth rates for several heats of SA-372 Grade J Class 70 steels (quench and tempered Cr-Mo steels) measured in gaseous hydrogen at pressure of 103 MPa. These data can be represented by the classic power-law formulation for fatigue crack growth:

$$(da/dN)_R = C_R \Delta K^m \quad (1)$$

where da/dN is the crack growth rate per cycle, C_R and m are constants and the subscript denotes a specific load ratio (R). Fatigue crack growth that follows this power-law dependence is often called stage II crack growth. This early data was limited to stress intensity factor range (ΔK) greater than 10 MPa $m^{1/2}$. More recent data has shown (Figure 2) that the fatigue crack growth

Sandia National Laboratories is a multimission laboratory managed and operated by National Technology & Engineering Solutions of Sandia, LLC, a wholly owned subsidiary of Honeywell International Inc., for the U.S. Department of Energy's National Nuclear Security Administration under contract DE-NA0003525.

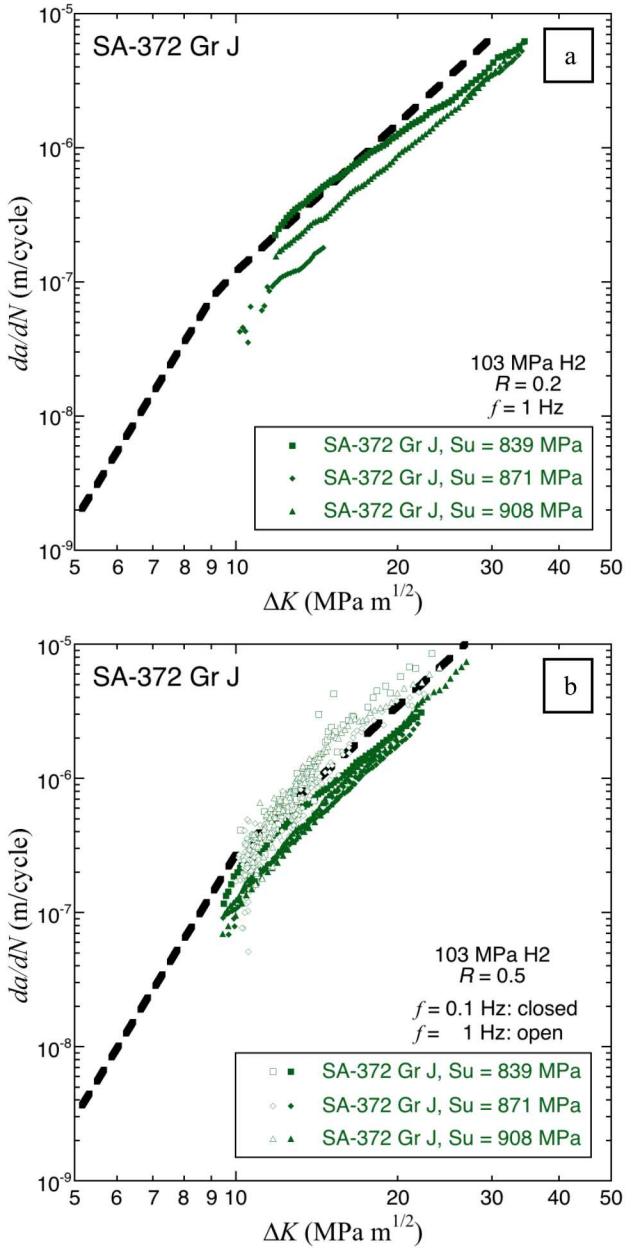

Figure 1. Fatigue crack growth rates of SA-372 Grade J steels in gaseous hydrogen at pressure of 103 MPa: (a) R = 0.2 [1] and (b) R = 0.5 [1, 2]. The dashed lines represent the master curve at the appropriate R.

response in gaseous hydrogen cannot be captured by a single power law over the entire range of ΔK [4, 5]. A pronounced inflection (or knee) in the da/dN-ΔK curve is typically observed near ΔK of 10 MPa m$^{1/2}$ for pressure vessel steels tested in high-pressure gaseous hydrogen. Thus, stage II fatigue crack growth can be separated into a low-ΔK regime and a high-ΔK regime. These two regimes can be independently represented by power laws, where the exponent m is greater in the low-ΔK regime. Consequently, if data is absent in the low-ΔK regime (as in Figure 1) and fatigue crack growth rates are inferred by extrapolation of trends from the high-ΔK regime, the fatigue crack growth rate is significantly overestimated, as shown in Figure 2.

Recently, fatigue crack growth rates in high-pressure gaseous hydrogen were reported for SA-372 Grade L and SA-723 steels (quench and tempered Ni-Cr-Mo steels) [3]. These new data included fatigue crack rates at lower ΔK than previously reported for SA-372 Grade J steels, exposing the knee of the fatigue response around ΔK of 10 MPa m$^{1/2}$. These developments led to a comprehensive review of the available data and the observation that the fatigue crack growth rates are relatively insensitive to the grade and heat of pressure vessel steel, at least for SA-372 and SA-723 steels with moderately low strength. Furthermore, it was determined that a relatively simple master curve provides an upper bound on fatigue crack growth rate for available data (within specific constraints). This master curve is the basis of Code Case 2938, which was approved by the ASME Board on Pressure Technology Code and Standards in 2018. This manuscript provides an overview of fatigue and fracture data measured in high-pressure gaseous hydrogen as well as a description of the master curve and technical basis for incorporation into Code Case 2938.

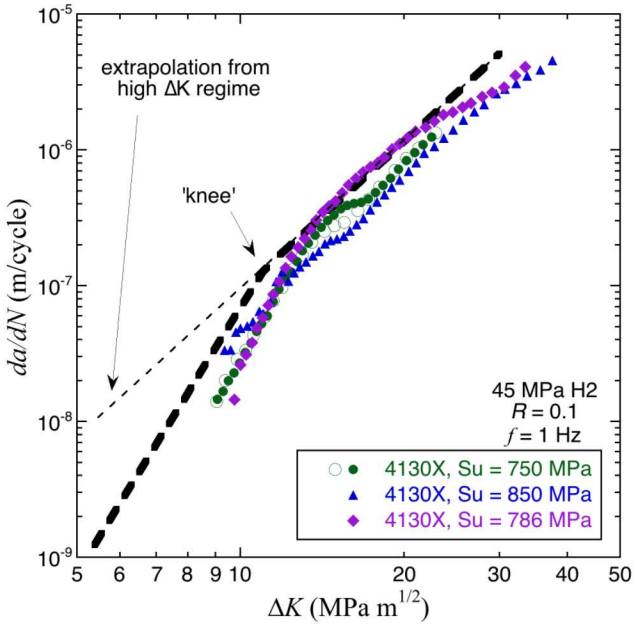

Figure 2. Fatigue crack growth rates of 4130X (Q&T Cr-Mo pressure vessel steel) in gaseous hydrogen at pressure of 45 MPa [4, 5]. The dashed line represents the master curve (at R = 0.1).

EXPERIMENTAL PROCEDURES

This manuscript does not provide new fatigue and fracture data in gaseous hydrogen. The goal here is to provide a critical assessment of data from previously published reports. However,

a brief summary of the materials and employed methods from this literature follows.

Materials

The primary focus of this work is pressure vessel steels, in particular quench and tempered (Q&T) Cr-Mo and Ni-Cr-Mo pressure vessel steels for hydrogen service at pressure near 100 MPa. The data used in the development of the master curve consists primarily of SA-372 Grade J Class 70 (Cr-Mo), SA-372 Grade L (Ni-Cr-Mo) and SA-723 Grade 1 and 3 (Ni-Cr-Mo). The SA-372 Grade L was also evaluated in an experimental heat treatment to produce a strength consistent with Grade J; this experimental heat treatment is referred to here as Grade L-LS. Both Grade L and Grade L-LS materials have the same composition. The yield strength (S_y) and tensile strength (S_u) of the Q&T steels are summarized in Table 1, representing 4 heats of SA-372 Grade J steel, one high-strength Cr-Mo steel (34CrMo4) and 3 heats of Ni-Cr-Mo steels (SA-372 Grade L and SA-723).

Fatigue and fracture data of other ferritic steels in gaseous hydrogen provide supplementary information [4, 5], but these data were not used directly in the development of the master curve. Several heats of 4130X pressure vessel steels, for example, were evaluated at lower pressure (Figure 2) to assess the use of transportable gas cylinders for hydrogen fuel tanks in mobile applications, as shown in Figure 2. Additionally, carbon steels for pipelines display fatigue and fracture behavior that is consistent with the behavior of pressure vessel steels, although testing of pipeline steels is typically performed at lower pressure [6-11]. The effect of pressure on the design curves will be discussed in a later section.

Fracture mechanics measurements

The testing equipment and methods for measuring environmentally-assisted fatigue crack growth and fracture resistance in high-pressure gaseous hydrogen are described elsewhere [3, 7, 12]. Briefly, typical compact tension specimens are used for measurement of fatigue crack growth rates (ASTM E647) and elastic-plastic fracture toughness (ASTM E1820). A commonly used geometry has a width (W) of 26.4 mm and thickness (B) of 12.7 mm.

While some work has used separate specimens for fatigue and fracture [1, 2, 13], current practice for in situ measurements in high-pressure gaseous hydrogen commonly utilizes the same test specimen for both measurements when possible [3, 14]. In other words, the fatigue crack growth test is conducted followed by the fracture toughness test on the same specimen. As such, the maximum stress intensity factor (K_{max}) during the fatigue test is managed to minimize the effects of fatigue-induced plasticity on the toughness measurement. The result is fatigue tests that emphasize relatively low K_{max} (<20 MPa m$^{1/2}$) and corresponding low ΔK. Conveniently, the low ΔK regime is arguably the most important portion of the fatigue crack growth curve as the majority of the cycle life occurs at the lower ΔK values.

For the data reported here, fatigue crack growth testing is most often conducted at a frequency of 1 Hz and load ratios (R) between 0.1 and 0.7. The majority of tests were conducted following standard procedures for constant load amplitude testing. However, acceleration of testing by control of the normalized K-gradient (γ) was also explored in Ref. [3]:

$$\gamma = \frac{1}{K}\frac{dK}{da} \tag{2}$$

where K is the applied stress intensity factor and a is the crack length. A negative K-gradient means that the ΔK is decreased as the crack grows (through a computer-controlled feedback loop where γ is the control channel), such that the fatigue crack growth rate (da/dN, crack growth per cycle, N) decreases over the course of the test segment. In contrast, in a constant load amplitude test, ΔK increases as the crack grows and the da/dN-ΔK curve is measured from low to high values of ΔK. Control of γ enables K-decreasing tests that probe lower ΔK values. The effect of γ on fatigue crack growth rate was determined to be negligible over the evaluated range from -0.4 to +0.4 mm^{-1} [3]. It is worth noting that testing time can also be significantly reduced in K-increasing tests with γ control in the range +0.2 to +0.4 mm^{-1} (with respect to constant load amplitude, where $\gamma \sim$ +0.1 mm^{-1}), especially for testing at low frequency ($f \leq 1$ Hz). More details are provided in Ref. [3].

The high fracture values of pressure vessel steels with $S_u < 915$ MPa in gaseous hydrogen generally require an elastic-plastic analysis. The reported values are determined from the intersection of the 0.2 mm offset blunting line with the JR curve (J-integral fracture resistance curve), consistent with conventional determination of J_{IC}. Monotonic loading is a distinguishing characteristic of the methods employed in these studies for the fracture resistance measurements in gaseous hydrogen, using the direct current potential difference (DCPD) method to monitor crack extension [15, 16]. The measured values for testing in gaseous hydrogen are referred to as J_H, or converted to units of stress intensity factor and referred to as K_{JH}. While the fracture methodology is consistent with a standard elastic-plastic fracture toughness measurement, values measured in gaseous hydrogen are generally referred to as fracture resistance to distinguish the measurement from a materials property (*i.e.*, fracture toughness) measured in air.

High-pressure hydrogen environments

All the testing considered in this overview was conducted at room temperature (20˚C). The Ni-Cr-Mo steels were tested in gaseous hydrogen at pressure of 106 MPa [3]. Data for SA-372 Grade J steels from Refs. [1, 2] were generated in gaseous hydrogen at pressure of 103 MPa. This small difference in pressure is insignificant considering the uncertainties associated with measurements in high-pressure environments as well as the variability in the response of the specimens in these environments.

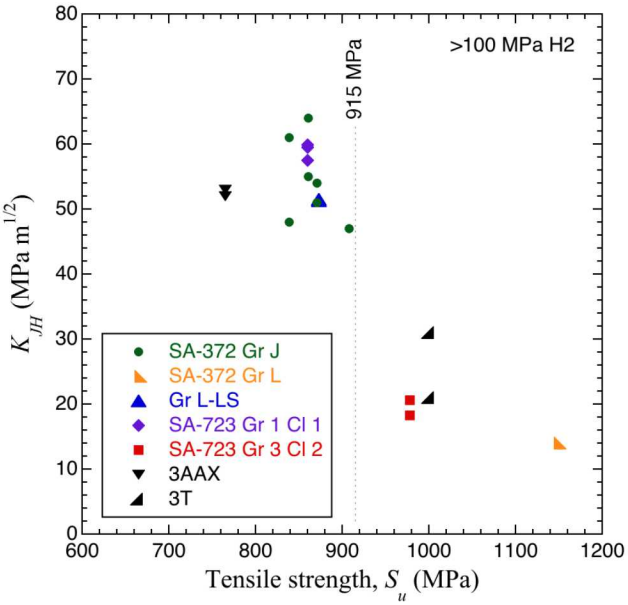

Figure 3. Fracture resistance (K_{JH}) as a function of tensile strength (S_u) for a variety of pressure vessel steels from Refs. [3, 15].

RESULTS AND DISCUSSION

Fracture resistance

The measured fracture resistance in high-pressure gaseous hydrogen are plotted in Figure 3 as a function of tensile strength for a number of pressure vessel steels from the literature [3, 15]. These data include steels from Table 1 as well as a few others. The steels with S_u < 915 MPa display K_{JH} > 40 MPa m$^{1/2}$, while the higher strength steels show fracture resistance less than about 20 MPa m$^{1/2}$. The significance of the fracture resistance should not be underestimated since low fracture resistance will affect the fatigue behavior. As K_{max} during a fatigue test approaches K_{JH}, the material response transitions to stage III fatigue crack growth, which is characterized by an acceleration of fatigue crack growth (*i.e.*, steeper slope of the *da/dN*-Δ*K* curve) and dependence on the load cycle and frequency. From a design point of view, stage III is generally undesirable. While transition to stage III fatigue behavior maybe not be an issue for most inert environments, in the presence of environmental effects, the rising load fracture resistance (K_{JH} as derived from ASTM E1820 methods) should not be ignored. Therefore, trends in fatigue crack growth should be informed by the fracture resistance of the material.

Fatigue crack growth

Fatigue crack growth rates used in the development of the master curve for high-pressure gaseous hydrogen service are reported in several studies: Cr-Mo [1, 2] and Ni-Cr-Mo [3]. The Cr-Mo steels were evaluated in load ratios of 0.2 and 0.5 and generally for ΔK > 10 MPa m$^{1/2}$ as shown in Figure 1. Fatigue

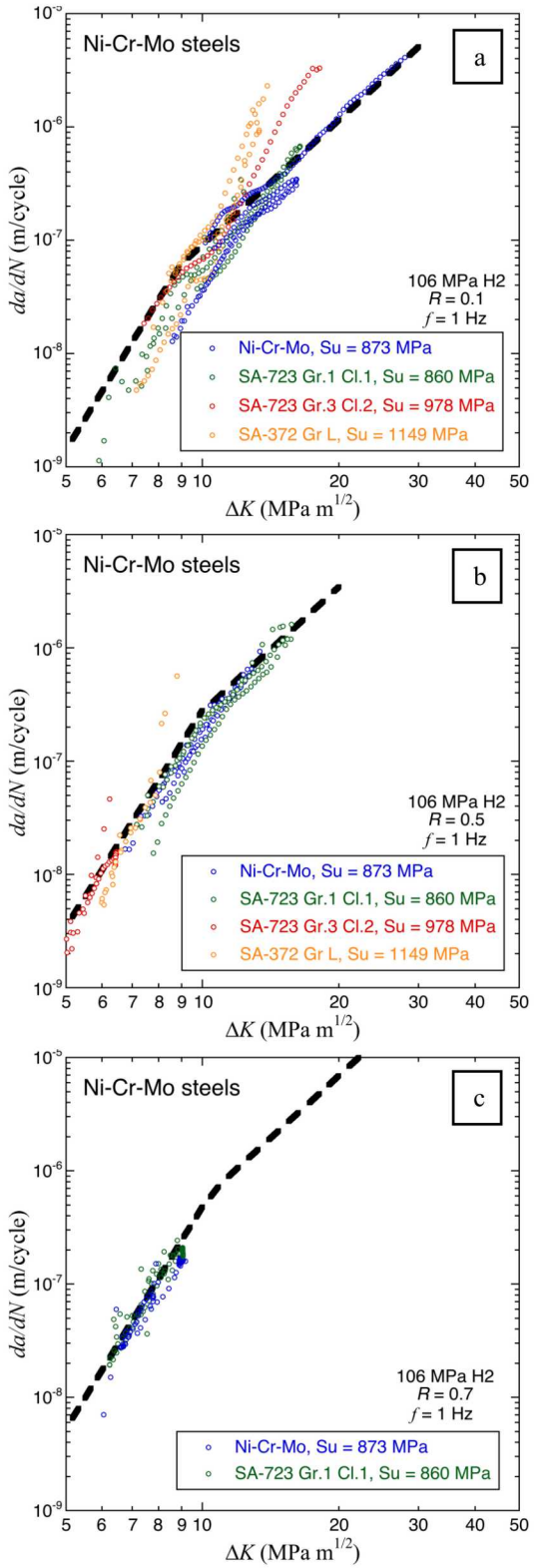

Figure 4. Fatigue crack growth rates of Ni-Cr-Mo steels in gaseous hydrogen from Ref. [3] at (a) R = 0.1, (b) R = 0.5, and (c) R = 0.7. The value of γ ranged from -0.4 to +0.4 mm^{-1}. The dashed lines represent the master curve.

crack growth rates of the Ni-Cr-Mo steels are shown in Figure 4 after Ref. [3]. While the evaluated ΔK range for the Ni-Cr-Mo steels depends on R, greater emphasis was placed on the low-ΔK regime in these more recent tests. Additionally, controlling the normalized K-gradient (γ) during these fatigue tests enabled access to lower values of ΔK.

In general, the fatigue crack growth rates are consistent for both Cr-Mo and Ni-Cr-Mo steels with $S_u < 915$ MPa ($K_{JH} > 40$ MPa m$^{1/2}$). The dashed line in the fatigue plots provides a consistent trend line for comparison of fatigue crack growth rate, emphasizing the overall similarity of the measured fatigue crack growth rate for these different materials and testing configurations. As will be discussed in the following section, these trend line represents the master curve, and accounts for effects of R.

The high-strength Ni-Cr-Mo steels are an exception to the bounding behavior of the master curve. In particular, the Ni-Cr-Mo materials with S_u greater than about 915 MPa deviate from the master curve at 'high' ΔK, displaying higher fatigue crack growth rates (Figures 4a and 4b). The transition to higher rates is attributed to the onset of stage III crack growth. As mentioned previously, the fracture resistance of the high strength steels is sufficiently low that K_{max} approaches K_{JH} during the fatigue cycling, causing acceleration of the crack growth rate. The transition from the master curve to stage III occurs at lower ΔK for $R = 0.5$, because K_{max} is higher for the same ΔK when R is higher:

$$K_{max} = \Delta K/(1 - R) \quad (3)$$

In high strength SA-723 steel (Grade 3, Class 2) and SA-372 Grade L steel, $K_{max} = 20$ MPa m$^{1/2}$ for $R = 0.5$ and $\Delta K = 10$ MPa m$^{1/2}$, which is about the measured fracture resistance (Figure 3). Therefore, the apparent fatigue response of the high-strength steels is significantly impacted by the low fracture resistance. Indeed, fatigue measurements of the high-strength Ni-Cr-Mo steels were not conducted at $R = 0.7$, since $K_{max} \sim K_{JH}$ even for ΔK as low as 5 MPa m$^{1/2}$.

High-strength Cr-Mo steels also show deviation from the master curve toward higher fatigue crack growth rate. As shown in Figure 5, high-strength 34CrMo4 (Q&T Cr-Mo pressure vessel steel with $S_u = 1045$ MPa) displays a higher fatigue crack growth rate than the master curve at $\Delta K \sim 24$ MPa m$^{1/2}$. In contrast, the master curve represents an upper bound on fatigue crack growth rate for the lower strength SA-372 Grade J from the same study [13].

The role of fatigue cycle frequency is also apparent in Figure 5. In general, the effect of frequency tends to saturate for frequency $\leq$1 Hz [13]. One obvious exception is the measurements on the high-strength 34CrMo4 steel at $\Delta K = 24$ MPa m$^{1/2}$. The enhanced effect of frequency in these data are indicative of the transition to stage III fatigue crack growth, as discussed above. Unfortunately, fracture resistance of the 34CrMo4 steel in gaseous hydrogen is not reported in Ref. [13], although the trend in Figure 5 suggests that K_{max} should approach

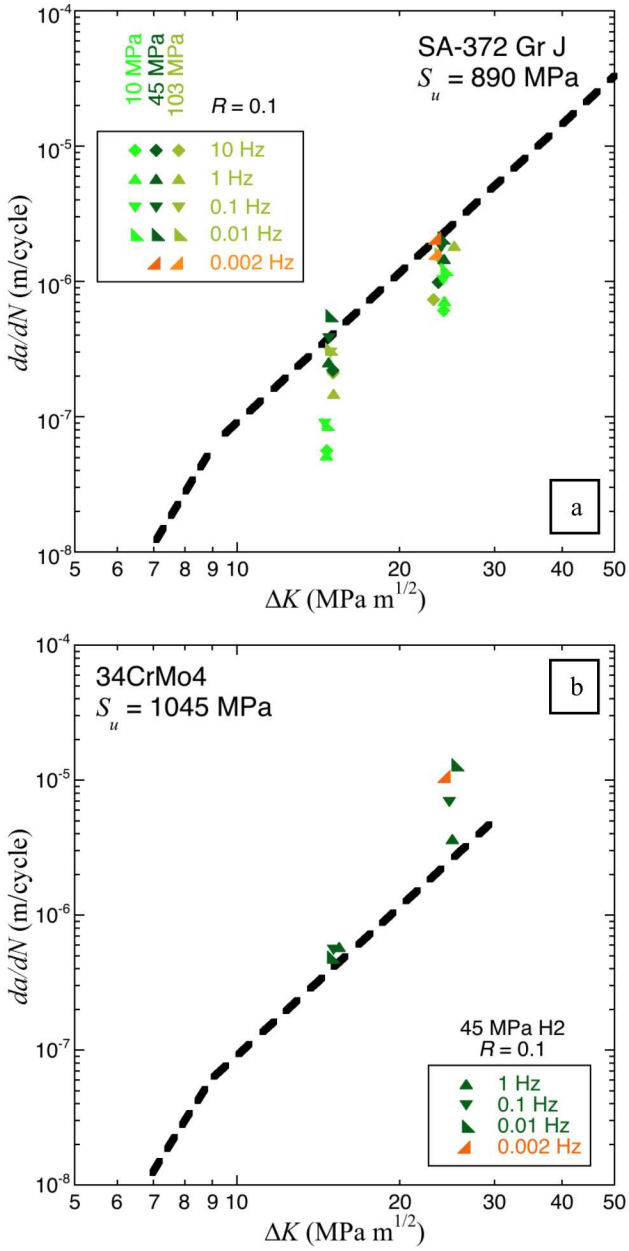

Figure 5. Fatigue crack growth rates at load ratio R = 0.1 for frequency between 0.002 and 10 Hz from Ref. [13]: (a) SA-372 Grade J, (b) 34CrMo4. Note the pressure of the tests for 34CrMo4 is 45 MPa. The dashed lines represent the master curve (R = 0.1).

(perhaps exceed) K_{JH} at $\Delta K \sim 24$ MPa m$^{1/2}$ for this steel (for which $S_u = 1045$ MPa).

In summary, the available fatigue crack growth data suggest that Cr-Mo and Ni-Cr-Mo steels display similar behavior in gaseous hydrogen when $S_u < 915$ MPa. This observation was the motivation for the development of a master curve to represent design information for pressure vessels in hydrogen service. The following section describes the development of the master curve

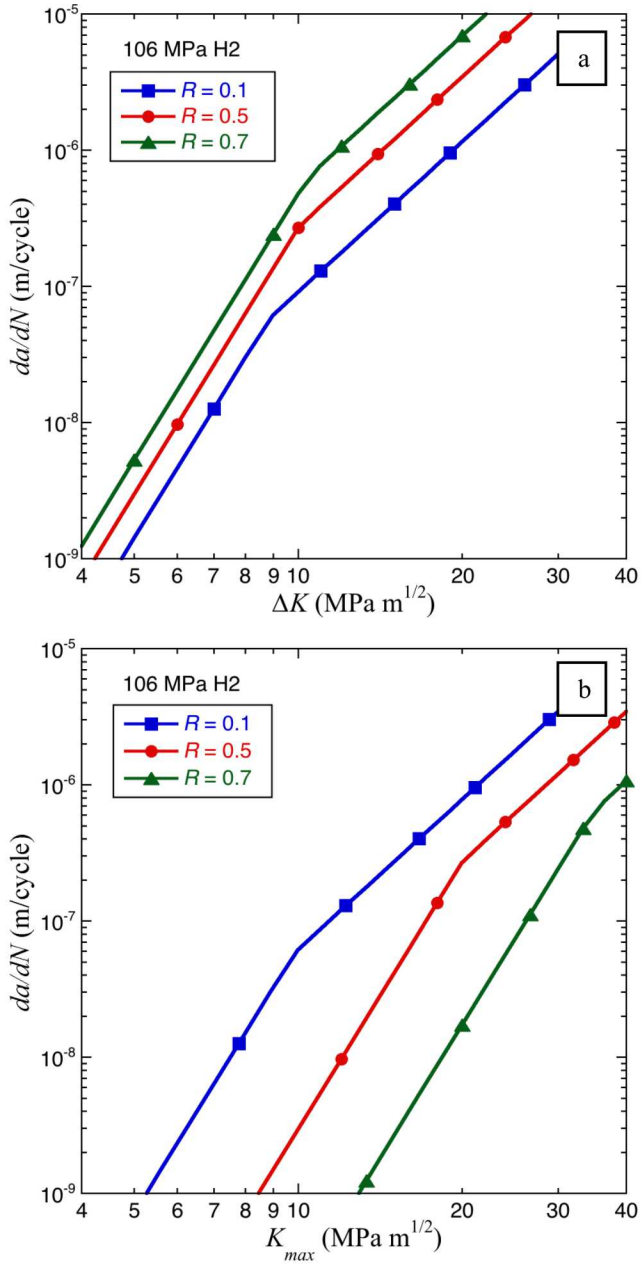

Figure 6. (a) Master curve representations of fatigue crack growth rate for several load ratios (from Equation 4). (b) Master curve as a function of K_{max} (to emphasize the relationship between ΔK, K_{max} and R).

and its limitations, which form the technical basis of Code Case 2938.

Development of master curves for ferritic steels

As described in the previous section, the data clearly show that low-strength steels consistently display similar fatigue crack growth rate in high-pressure gaseous hydrogen. Additionally, a master curve can be derived that captures the effect of R as well as the knee in the *da/dN*-ΔK curves, as indicated by the dashed lines in plots of fatigue crack growth rate. To establish the master curve, the data for the Ni-Cr-Mo steels was generalized to a self-consistent formulation:

$$da/dN = C\left[\frac{1+C_H R}{1-R}\right]\Delta K^m \quad (4)$$

such that the exponent m is independent of the load ratio (R), while C and C_H are constants. Due to the knee in the *da/dN*-ΔK curves (e.g., Figure 2), two sets of constants are needed, as well as a means to quantitatively determine the knee as a function of R. Equation 1 is used to fit the data for the low-ΔK regime and high-ΔK regime independently for each value of R, with m constant for each ΔK regime. By curve fitting C_R to the functional form:

$$C_R = C\left[\frac{1+C_H R}{1-R}\right] \quad (5)$$

both C and C_H can be determined for both the low-ΔK regime and the high ΔK-regime. Constants for the relationship in Equation 4 (and Equation 5) are provided in Table 2. Examples of the predicted fatigue crack growth curves at different load ratios are shown in Figure 6a. In addition to the traditional plot of crack growth rate versus ΔK, a plot of the same information is plotted in Figure 6b as function of K_{max} (Equation 2 relates ΔK to K_{max}). For the same loading condition (pressure) and defect size in a pressure vessel, K_{max} will be independent of R (while ΔK is not). As shown in Figure 6b, for the same K_{max}, the fatigue crack growth rate with $R = 0.7$ can be more than two orders of magnitude lower than at $R = 0.1$.

It is important to emphasize that these curves were developed to capture stage II crack growth. For high strength steels, where K_{JH} in gaseous hydrogen can be as low as 20 MPa m$^{1/2}$, the master curve does not capture the fatigue behavior, as discussed in the previous section. Therefore, these relationships be used only for SA-372 and SA-723 steels with S_u < 915 MPa and in the limit that K_{max} < 40 MPa m$^{1/2}$. The latter criterion essentially restricts the use of the master curve to loading conditions where K_{JH} is not exceeded.

The knee in the *da/dN*-ΔK curve is determined by equating the *da/dN* relationships (Equation 1) for the low-ΔK and high-ΔK regimes at specific values of R and solving for ΔK. The value of ΔK at the knee is defined as ΔK_c and is a function of R only. In other words, for a given value of R, ΔK_c is determined from

$$C_{R,L}(\Delta K_c)^{m_L} = C_{R,H}(\Delta K_c)^{m_H} \quad (6)$$

where the subscripts L and H refer to the constants from the low-ΔK regime and the high-ΔK regime respectively. A second order polynomial captures the evolution of ΔK_c as a function of R:

$$\Delta K_c\left[\text{MPa m}^{1/2}\right] = 8.475 + 4.062R - 1.696R^2 \quad (7)$$

where ΔK_c is in units of MPa m$^{1/2}$.

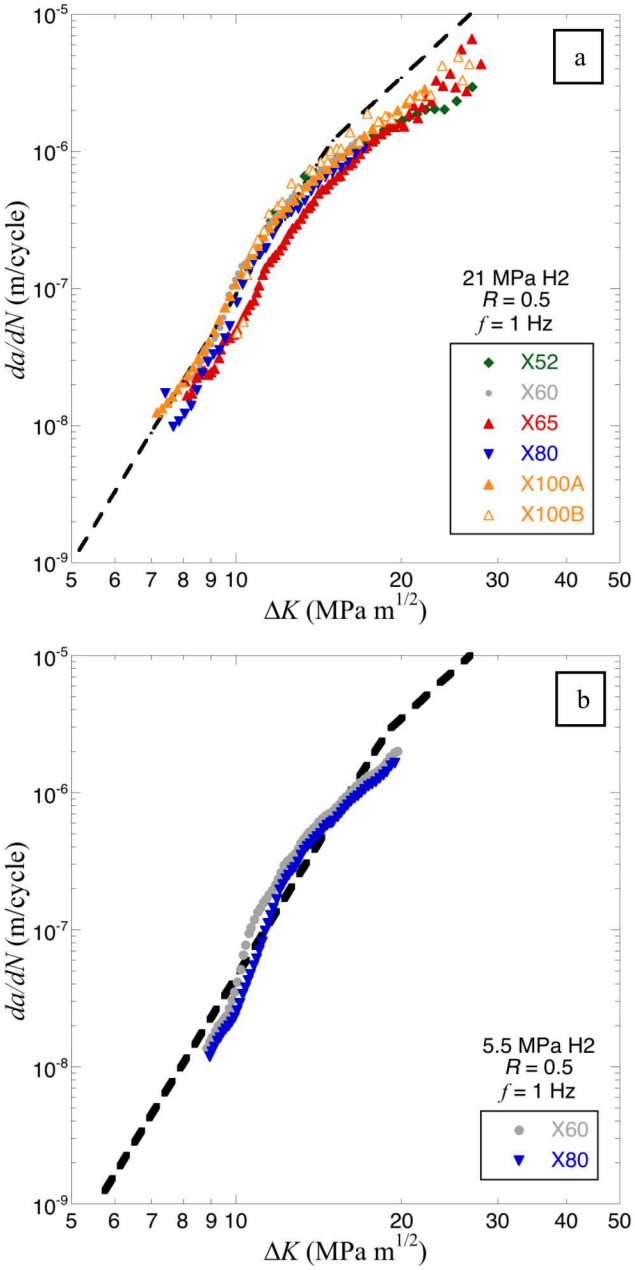

Figure 7. Fatigue crack growth rates of pipeline steels with R = 0.5 at pressure of (a) 21 MPa and (b) 5.5 MPa. The dashed lines are derived from the master curves for pressure vessel steels for the specific load ratio (R = 0.5) and pressure of these data sets. [7-11].

While the fatigue crack growth curves were developed primarily from the testing of the Ni-Cr-Mo pressure vessel steels, these curves are consistent with the literature data for Cr-Mo pressure vessel steels as shown in Figures 1 and 5a (the material represented in Figure 5b does not meet restriction on tensile strength). This assessment provides the technical basis for the master curve, which replaces the need for extensive materials testing in high-pressure gaseous hydrogen, at least within described bounds on steels, strength and K_{max}.

Application to Code Case 2938

Code Case 2938 was recently developed to complement ASME Boiler and Pressure Vessel Code Section VIII Division 3 by formalizing the master curve concept for fatigue crack growth in high-pressure gaseous hydrogen. Article KD-10 (BPVC VIII-3) requires extensive fatigue testing of pressure vessel steels to inform design of high-pressure gaseous hydrogen transport and storage vessels. The data in this report for SA-372 and SA-723 steels shows remarkable consistency in the fatigue crack growth response of the steels within well-defined constraints (as outlined below). Moreover, a critical assessment of the data shows that a relatively simple master curve represents well the fatigue behavior of this class of steels over a wide range of R and ΔK. The resulting master curve is the basis for the design curve incorporated into Code Case 2938, which applies to SA-372 and SA-723 steels along with the restriction on applicability as follows:

(a) The crack growth rate at the deepest point on the crack periphery (da/dN) shall be a function of the range of stress intensity factor (ΔK), as given by Equation 4.

(b) For $K_{min} \leq 0$, the value of K_{min} shall be set to 0 in all equations (K_{min} represents the minimum stress intensity in the load cycle).

(c) The operating pressure shall not exceed 103 MPa (15 ksi).

(d) The maximum measured tensile strength of the steel shall not exceed 915 MPa (133 ksi).

(e) K_{max} shall not exceed 40 MPa m$^{1/2}$ (36 ksi in$^{1/2}$).

Pressure dependence

While not included in Code Case 2938, preliminary analysis suggests that the master curve can be adapted for similar carbon and low-alloy ferritic steels at lower pressure (*e.g.*, <106MPa). The master curve can be extended to capture the effects of pressure by adding an empirical fugacity term as

$$da/dN = C\left[\frac{1+C_H R}{1-R}\right]\Delta K^m \left(\frac{f}{f_{ref}}\right)^{1/2} \quad (8)$$

where f is the fugacity of hydrogen at the pressure of interest, and f_{ref} is the fugacity at the reference pressure, while the constants remain the same. For pressure of 106 MPa, f_{ref} is 211 MPa (see Ref. [17] for discussion of fugacity and square root dependence). However, this correction for pressure only applies to the low ΔK-regime based on empirical evidence. In the high-ΔK regime, da/dN appears to be independent of pressure, as shown in Figure 2 where the pressure correction (Equation 8) is only applied to the low-ΔK regime. Examples of the pressure-corrected master curve is plotted in Figure 7 along with fatigue crack growth rate data for pipeline steels at two different

pressures (5.5 and 21 MPa). These results suggest that a single master curve can potentially be adopted for a wide range of pressure vessel and pipeline steels for (i) load ratios at least between 0 and 0.7, and (ii) any pressure of gaseous hydrogen relevant to fuel cell technology (at ambient temperature). More study is needed to clarify the apparent difference of pressure dependence in the low- and high-ΔK regimes.

SUMMARY

Code Case 2938 provides a relatively simple empirical relationship for fatigue analysis of SA-372 and SA-723 steels in high-pressure hydrogen storage vessels. The master curve uses a two-part power law to capture the observed fatigue crack growth response of these steels at high and low ΔK respectively. Extensive data for SA-372 and SA-723 measured in high-pressure (~100 MPa) gaseous hydrogen have been used to develop and validate the master curve. However, it has been shown that pressure vessel steels with tensile strength greater than 915 MPa show accelerated crack growth relative to the master curve. Low fracture resistance of high-strength steels appears to contribute to the accelerated fatigue crack growth as a result of transition to stage III fatigue crack growth. For these reasons, application of the master curve has three practical and important limitations:

- $S_u < 915$ MPa
- Gaseous hydrogen pressure ≤ 103 MPa
- $K_{max} < 40$ MPa $m^{1/2}$.

Additionally, preliminary evidence suggests that the master curve can be modified by adding a simple term to normalize for the desired hydrogen fugacity. Although the pressure term was not incorporated in the Code Case, literature data suggest that the fatigue behavior of pressure vessel and pipeline steels can be captured at lower pressure with this modification.

ACKNOWLEDGMENTS

The authors are grateful to J. Campbell and B. Davis for support of high pressure testing. Sandia National Laboratories is a multimission laboratory managed and operated by National Technology and Engineering Solutions of Sandia, LLC., a wholly owned subsidiary of Honeywell International, Inc., for the U.S. Department of Energy's National Nuclear Security Administration under contract DE-NA-0003525.

REFERENCES

1. B.P. Somerday, C. San Marchi and K. Nibur, Measurement of fatigue crack growth rates for SA-372 Gr. J steel in 100 MPa hydrogen gas following article KD-10 (PVP2013-97455), Proceedings of the ASME Pressure Vessels and Piping Division Conference, Paris, France, 14-18 July 2013.
2. B.P. Somerday, K.A. Nibur and C. San Marchi, Measurement of fatigue crack growth rates for steels in hdyrogen containment components, Proceedings of the International Conference on Hydrogen Safety (ICHS), Ajaccio, Corsica, France, September 2009.
3. C. San Marchi, P. Bortot, Y. Wada and J.A. Ronevich, Fatigue and fracture of high-hardenability steels for thick-walled hydrogen pressure vessels, Proceedings of the International Conference on Hydrogen Safety (ICHS), Hamburg, Germany, 11-13 September 2017.
4. C. San Marchi, D. Dedrick, P. Van Blarigan, B. Somerday and K. Nibur, Pressure cycling of type 1 pressure vessels with gaseous hydrogen, Proceedings of the International Conference on Hydrogen Safety (ICHS), San Francisco CA, 12-14 September 2011.
5. C. San Marchi, A. Harris, M. Yip, B.P. Somerday and K.A. Nibur, Pressure cycling of steel pressure vessels with gaseous hydrogen (PVP2012-78709), Proceedings of the ASME Pressure Vessels and Piping Division Conference, Toronto, Ontario, Canada, 15-19 July 2012.
6. C. San Marchi, B.P. Somerday, K.A. Nibur, D.G. Stalheim, T. Boggess and S. Jansto, Fracture resistance and fatigue crack growth of X80 pipeline steel in gaseous hydrogen (PVP2011-57684), Proceedings of the ASME Pressure Vessels and Piping Division Conference, Baltimore MD, July 2011.
7. C. San Marchi, B.P. Somerday, K.A. Nibur, D.G. Stalheim, T. Boggess and S. Jansto, Fracture and fatigue of commercial grade pipeline steels in gaseous hydrogen (PVP2010-25825), Proceedings of the ASME Pressure Vessels and Piping Division Conference, Bellevue WA, 18-22 July 2010,
8. B.P. Somerday, P. Sofronis, K.A. Nibur, C. San Marchi and R. Kirchheim, Elucidating the variables affecting accelerated fatigue crack growth of steels in hydrogen gas with low oxygen concentrations, Acta Mater 61 (2013) 6153–6170.
9. A.J. Slifka, E.S. Drexler, N.E. Nanninga, Y.S. Levy, D. McColskey, R.L. Amaro and A.E. Stevenson, Fatigue crack growth of two pipeline steels in a pressurized hdyrogen environment, Corros Sci 78 (2014) 313-321.
10. J.A. Ronevich, B.P. Somerday and C. San Marchi, Effects of microstrucutre banding on hydrogen assisted fatigue crack growth in X65 pipeline steels, Intern J Fatigue 82 (2016) 497-504.
11. J.A. Ronevich, C.R. D'Elia and M.R. Hill, Fatigue crack growth rates of X100 steel welds in high pressure hydrogen gas considering residual stress effects, Eng Fract Mech 194 (2018) 45-51.
12. B.P. Somerday, J.A. Campbell, K.L. Lee, J.A. Ronevich and C. San Marchi, Enhancing safety of hydrogen containment components through materials testing under in-service conditions, Int J Hydrogen Energy 42 (2017) 7314-7321.
13. B.P. Somerday, P. Bortot and J. Felbaum, Optimizing measurement of fatigeu crack growth relationships for Cr-Mo pressure vessl steels in hydrogen gas (PVP2015-45424), Proceedings of the ASME Pressure Vessels and Piping Division Conference, Boston MA, 19-23 July 2015.
14. K.A. Nibur, C. San Marchi and B.P. Somerday, Fracture and fatigue tolerant steel pressure vessels for gaseous hydrogen (PVP2010-25827), Proceedings of the ASME Pressure

Vessels and Piping Division Conference, Bellevue WA, 18-22 July 2010.
15. K.A. Nibur, B.P. Somerday, C. San Marchi, J.W.I. Foulk, M. Dadfarnia, P. Sofronis and G.A. Hayden, Measurement and interpretation of threshold stress intensity factors for steels in high-pressure hydrogen gas (SAND2010-4633), Sandia National Laboratories, Livermore CA, 2010.
16. K.A. Nibur, B.P. Somerday, C. San Marchi, J.W. Foulk III, M. Dadfarnia and P. Sofronis, The relationship between crack-tip strain and subcritical cracking thresholds for steels in high-pressure hydrogen gas, Metall Mater Trans 44A (2013) 248-269.
17. C. San Marchi, B.P. Somerday and S.L. Robinson, Permeability, Solubility and Diffusivity of Hydrogen Isotopes in Stainless Steels at High Gas Pressure, Int J Hydrogen Energy 32 (2007) 100-116.

Table 1. Strength of the steels used to establish the basis for the master curve for fatigue crack growth in high-pressure gaseous hydrogen.

Material	Yield strength, S_y (MPa)	Tensile strength, S_u (MPa)	Reference
Cr-Mo Q&T pressure vessel steels			
SA-372 Grade J Class 70	642	839	[1, 2]
SA-372 Grade J Class 70	731	871	[1, 2]
SA-372 Grade J Class 70	784	908	[1, 2]
SA-372 Grade J Class 70	760	890	[13]
34CrMo4	850	1045	[13]
Ni-Cr-Mo Q&T pressure vessel steels			
SA-372 Grade L	1053	1149	[3]
SA-372 Grade L–LS	731	873	[3]
SA-723 Grade 1 – Class 1	715	860	[3]
SA-372 Grade 3 – Class 2	888	978	[3]

Table 2. Fatigue crack growth rates in high-pressure gaseous hydrogen: constants for Equation 4.

	da/dN low-ΔK regime $\Delta K < \Delta K_c$	*da/dN* high-ΔK regime $\Delta K \geq \Delta K_c$
C (m/cycle)	3.5×10^{-14}	1.5×10^{-11}
C_H (no units)	0.4286	2.0
m (no units)	6.5	3.66